Investigation on Mechanical Damage of No-Insulation REBCO Pancake Coil by Multi-Physics Quench Simulation

Shumpei Mori and So Noguchi

***Abstract*— A no-insulation (NI) winding technique greatly improves the thermal stability of $REBa_2Cu_3O_x$ (RE=Rare Earth; REBCO) pancake coils. Since it has recently been pointed out that strong electromagnetic forces due to induced currents cause mechanical damage to NI REBCO coils during quench propagation under high magnetic field. The mechanical stability must be investigated and discussed further. We have developed a multi-physics quench simulation for NI REBCO pancake coils by combining a 2D stress/strain finite element analysis (FEA) with an electromagnetic field analysis of partial element equivalent circuit (PEEC) method and a 2D thermal FEA. The simulation results showed the consistency with the experimental results.**

***Index Terms*—Elastic analysis, mechanical damage, multi-physics simulation, no-insulation winding technique, REBCO coil.**

I. Introduction

In recent years, pancake coils wound with $REBa_2Cu_3O_x$ (REBCO, RE = Rare Earth) tapes are expected to be applied to devices that require a high magnetic field due to their excellent mechanical and critical current density characteristics. In addition, by applying a no-insulation (NI) winding technique to REBCO pancake coils, the thermal stability of REBCO pancake coils is greatly enhanced [1]–[3]. The NI winding technique, where an insulator between the turns is removed, prevents currents from flowing into a normal-state-transitioned zone, because an operating current carries directly into the adjacent turns. As a result, REBCO magnets can be prevented from burning-out, and the thermal stability is greatly improved [4], [5]. Many researchers have recently focused on mechanical damage in NI REBCO magnets [6]–[8]. It is, further, necessary to understand the transient electromagnetic and mechanical phenomenon when a normal-state transition occurs. Because, the strong electromagnetic force under a high magnetic field due to an induced current during quench propagation probably causes a mechanical damage of REBCO tapes and deterioration of the critical current [9]–[14]. An electromagnetic, thermal, and mechanical multi-physics analysis method is required to be developed in order to compute the magnetic field and the current of NI REBCO magnets in detail, because the accurate strains and stresses of NI REBCO magnets is needed in order to evaluate the mechanical stability.

This work was supported by the JSPS KAKENHI under Grant No. 20H02125. *(Corresponding author: So Noguchi.)*

S. Mori and S. Noguchi are with the Graduate School of Information Science and Technology, Hokkaido University, Sapporo 060-0814, Japan. (e-mail: s_mori@em.ist.hokudai.ac.jp, noguchi@ssi.ist.hokudai.ac.jp).

We have developed a multi-physics simulation code for accurate quench simulation by combining 2-D stress/strain finite element analysis (FEA) with electromagnetic analysis of partial equivalent electrical circuit (PEEC) method and 2-D thermal FEA [2], [15], [16]. In this paper, quench simulations of 12-stacked NI REBCO single pancake coils were performed on a few different conditions to investigate the stress/strain behaviors of the NI REBCO coils. The mechanism of quench propagation and the factors of mechanical damage of each coil are discussed.

II. Simulation Method

In the developed multi-physics analysis of NI REBCO pancake coil, an electromagnetic analysis is coupled with a stress/strain and a thermal analysis as shown in Fig. 1. The current behavior is computed with the PEEC method [2], [15], [16]. The thermal analysis with 2-D finite element method (FEM) is performed as an input of the Joule heating computed by PEEC method, and also the stress/strain analysis with 2-D FEM as an input of the BJR stress.

In the PEEC model, the NI REBCO pancake coils are represented by a great number of subdivided azimuthal elements. Each element consists of a local self/mutual inductance and a REBCO tape resistance, which are connected a radial contact resistance in parallel. The equivalent electric resistance of REBCO layer in this PEEC is modeled with the power index model, where the critical current was derived from the experiments [17]. The critical currents on each partial element in PEEC was computed depending on the locally experienced magnetic fields, and they changed with the time-varying magnetic fields and temperatures.

The stress/strain analysis was performed with 2-D FEM using four-node isoparametric elements on the $r\theta$ plane. The governing equation [18] to be solved is as follows:

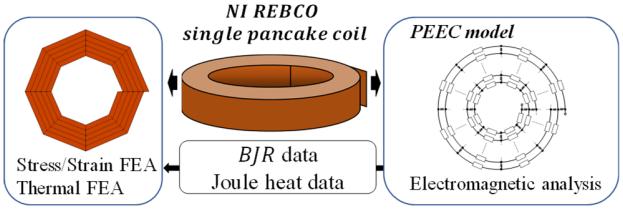

Fig. 1. Multi-physics NI REBCO pancake coil simulation, coupling electromagnetic, stress/strain, and thermal analysis.

$$r\frac{\partial \sigma_r}{\partial r}+\frac{\partial \tau_{r\theta}}{\partial \theta}+\sigma_r-\sigma_\theta+rJ_\theta B_z=0 \quad (1)$$

where r, σ_r, σ_θ, $\tau_{r\theta}$, J_θ, and B_z are the radial position, the radial and hoop stresses, the shear stress around z-axis, the azimuthal current, and the z component of magnetic field, respectively. B_z, J, and r of each element are obtained from the electromagnetic analysis of PEEC method. The strains ϵ_r and ϵ_θ in the r and θ directions are given by

$$\epsilon_r=\frac{\sigma_r}{E_r}-\nu\frac{\sigma_\theta}{E_\theta} \quad (2)$$

$$\epsilon_\theta=\frac{\sigma_\theta}{E_\theta}-\nu\frac{\sigma_r}{E_r} \quad (3)$$

where E_r and E_θ are the Young's modulus, respectively, in the r and θ directions, and ν is the Poisson's ratio [19]. As a boundary condition, $\sigma_r=0$ is given on the inner and outer surfaces of each pancake coil.

III. Simulation Results

Table I lists the specifications of the simulated NI REBCO magnet consisting of 12 single pancake (SP) coils, as shown in Fig. 2. Every pancake coil is wound with REBCO tape using the NI winding technique. In this paper, the critical strain of REBCO tape is assumed to be 0.45% [21]. It has also been reported that the critical current of REBCO tape degrades when the REBCO tape experiences a large strain [10]; however, this critical current degradation due to stress is not considered in this present simulation, because the critical current degradation mechanism is not yet completely clear.

Table II lists the simulation conditions. In this simulation, it is assumed that an external magnetic field of 13.5T is applied in the z direction by an outsert magnet.

We performed quench simulations of the NI REBCO pancake coils on three different conditions (cases A, B, and C) as shown in Table III, and analyzed them multi-physically. In the case A, one element on 50th turn of SP #1 is initially transitioned into normal state at the operating currents of 450 A. The operating current is 300 A in the case B, and the initial quench condition is the same as the case A. In the case C, all the elements of SP #1 are simultaneously transitioned into a normal state, and the operating currents is 450 A. Here, as the simulation process of the local initial normal-state transition, the REBCO layer resistances were changed to the normal-state

TABLE I
Specifications of NI REBCO Coils and REBCO Tapes

Number of SPs	12
Coil i.d.; o.d. (mm)	120.0; 158.4
Distance between each pancake (mm)	1.0
Total coil height (mm)	59.0
Number of turns	100
Contact resistivity ($\mu\Omega\cdot cm^2$)	70.0 [20]
Magnet constant (mT/A)	9.98
Azimuthal division number	8
Total element number	800×12
Tape width (mm)	4.0
Tape thickness (mm)	0.1
REBCO layer thickness (μm)	1.0
Copper matrix thickness (μm)	20 (each side)
Critical current at 77 K, s.f. (A)	115
n index	30
Young's modulus E_r; E_θ (GPa)	130; 130
Poisson's ratio	0.4

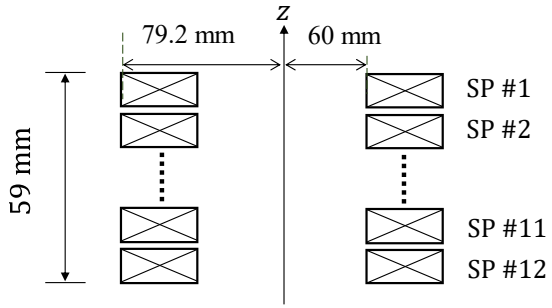

Fig. 2. Simulation model of NI REBCO magnet consisting of 12 single pancake coils (SPs #1-#12).

TABLE II
Simulation Conditions

Operating temperature (K)	20
External field (T)	13.5
Operating current (A)	450, 300
Time step in simulation (ms)	1

TABLE III
Quench Simulation Conditions

Case	A	B	C
Operation current (A)	450	300	450
Initial normal state transition occurrence	One element on 50th turn in SP #1	One element on 50th turn in SP #1	all elements in SP #1

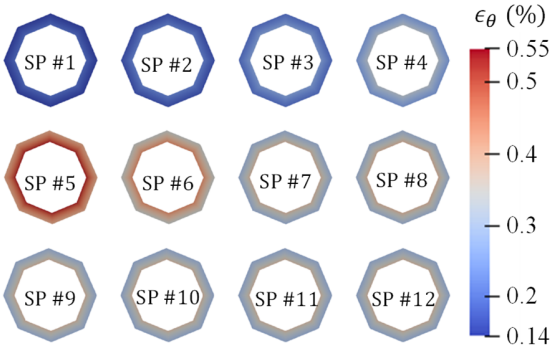

Fig. 3. Strain distribution on each SP at t = 0.02 s in case A.

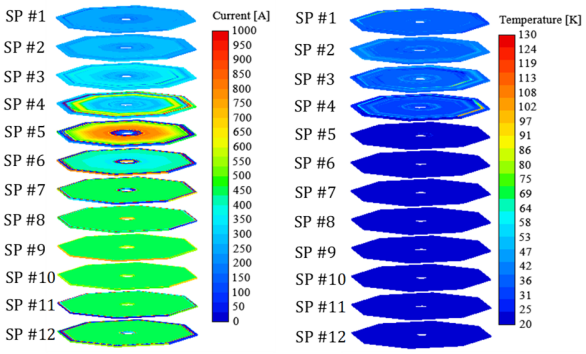

Fig. 4. (a) Azimuthal current and (b) temperature distribution at t = 0.02 s in case A.

values.

In all the cases, the operating current is constant during the quench simulations.

A. Simulation results of multi-physics quench simulation

Figs. 3 and 4 show the distributions of strain, azimuthal current, and temperature at t = 0.02 s in the case A. As shown in Fig. 4(b), the coil temperature reaches to 130 K at t = 0.02 s. The radial currents increase with the induced currents which increase with quench propagation. The radial currents through turn-to-turn contact surfaces produce the Joule heat, subsequently the temperature rises to 130 K. The temperature of 130 K is high enough that the coils transition into the normal state, but small enough that the coils do not burn out. Therefore, the magnet is thermally stabilized. Meanwhile, in Fig. 3, a large strain appears in SP #5, and it may cause the coil to be mechanically damaged. This large strain is generated by the high induced current due to quench propagation from SP #1 to #4. i.e., the high-field NI REBCO coils are highly thermally stable; nevertheless, they would be mechanically damaged due to a high induced current when quench propagation occurs from one pancake coil to other coils.

B. Comparison Between Each Case

Fig. 5 shows the time transition of maximum strain on each SP coil in case A, B, and C.

In the case A, after t = 0 s, the maximum strain on every coil changes. The strain on the initially quenched SP #1 decreases as a normal zone propagates inside the coil. By contrast, the strain on SPs #2-#11 increases, because they have a large current induced by the normal-state-transitioned coils. Note that, since the maximum strain values of SPs #3 to #10 are higher than the critical strain of 0.45%, they have a high probability of mechanical damage. Meanwhile, the strain on SP #12 decreases from t = 0.02 s.

In the case B, no change in strain can be seen after the local normal-state transition on the 50th turn of SP #1. Due to the low operating current, the quench propagation does not occur. It denotes that the mechanical stability of the NI REBCO magnet is maintained even when a local normal-state transition happens.

In the case C, the normal zone propagates faster than the case A. The large strains exceeding the critical strains occur in SPs #3-#10 like the case A. However, the large strain on SP #2 can also be seen, differently from the case A.

We, in the next section, discuss the facts that the strain reduction in SP #12 begins before the strain increases in SP #6-#9, and that the strain of SP #2 in the case A is small enough not to be mechanically damaged.

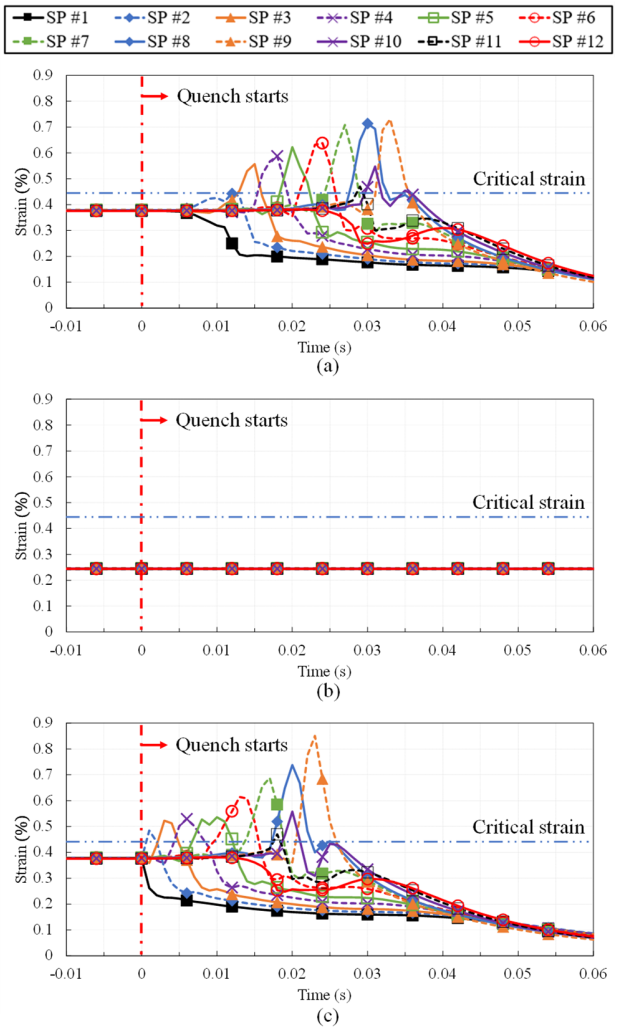

Fig. 5. Time transition of maximum strain on each SP coil in the cases (a) A, (b) B, and (c) C.

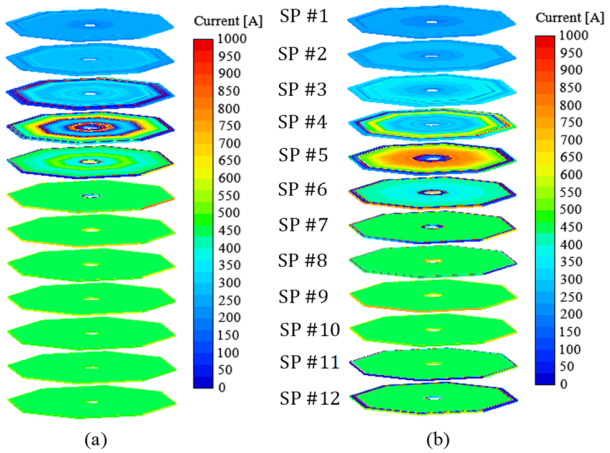

Fig. 6. Circumferential current maps at (a) t = 0.016 s and (b) t = 0.020 s in case A.

IV. Discussions

A. Decrease in Strain on SP #12

In Figs. 5(a) and (c), the strain of SP #12 begins decreasing at 0.02 s and 0.01 s, respectively. Figs. 6(a) and (b) individually show the distribution of the azimuthal current at t = 0.016 s and 0.020 s in the case A. The current starts being induced at the outermost turn of SP #12 at 0.016 s, and then increases further; eventually a local normal zone appears at 0.02 s; nevertheless a local normal zone does not occur in the SPs #9, #10, and #11 at that time. Afterwards, the normal zone propagates upward from the bottom SP #12. As a result, the quench propagates from both

the top and bottom of the magnet, as illustrated in Fig. 8. The same quench-propagation phenomenon can be observed in the case C. The cause of the local normal-state appearance is the increase in the magnetic field. With approaching the high induced current from the top to the lower coils, the magnetic field on SP #12 increases; the radial and axial magnetic field magnitude in SP #12 increase by 22 mT and 80 mT from 0.016 s to 0.020 s, respectively. The increase of the magnetic field and the induced current resulted in the local normal zone on the outermost turn of SP #12.

Consequently, the strain of SPs #1 and #12 decreases without experiencing a mechanical damage, because they have no induced current due to quench propagation from the adjacent pancake coils.

B. Cause of Small Strain on SP #2 in Case A

As shown in Fig. 5(a), in the case A, the strain on SP #2 is clearly smaller than that of the other middle coils (SPs #3-#10), in spite of the current induced in SP #2 by the normal-state transition of SP #1. In the case A, the normal-state propagation proceeds simultaneously on SPs #1 and #2, as shown in Fig. 7. Fig. 7 shows the azimuthal current at $t = 0.008$ s in the case A. Since the initial local normal-state transition occurs on the middle turn of SP #1, a current is induced in the middle turns of SP #2 as well as the neighbor turns of SP #1. The induced currents propagate the normal zone in SPs #1 and #2 at the same time. Accordingly, the induced current is large enough to propagate the normal zone, but too small to mechanically damage the pancake coils. By contrast, in the case C, a current large enough to mechanically damage is induced in SP #2 immediately after the whole SP #1 reaches to quench at $t = 0$.

Similarly, for SP #11, the outermost turn of SP #12 transitions into a normal state before the quench of SP #11. Afterwards, the simultaneous normal-state propagation in SPs #11 and 12 happens. This phenomenon is the reason why the strain of SPs #2 and #11 in the case A is smaller than that of the other middle pancake coils. This phenomenon is consistent with experimental facts observed in the 45.5-T generation [12]. No damage was observed in the second single pancake coils from the top and bottom in the post-mortem measurement of the REBCO tape critical current. As the simulation model and conditions in this paper are different from those in [12], the validity of this consistent phenomenon should be, in detail, investigated in near future.

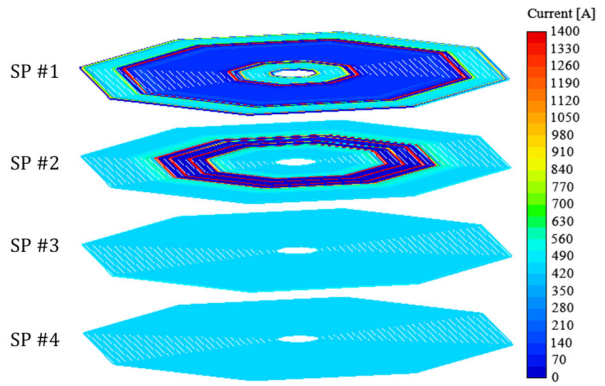

Fig. 7. Circumferential current distribution on the top 4 SPs at $t = 0.008$ s in case A.

As mentioned above, the middle SP coils (#3-#10) are mechanically damaged because of a large induced current, in the case A. Meanwhile, it was reported that the top and bottom SP coils were probably damaged due to a screening current [22]. As illustrated in Fig. 9, in a high magnetic field magnet consisting of insert stacked pancake coils and outsert coils, there is a low possibility that the second pancake coils from the top and bottom are damaged, whereas the other pancake coils are highly possibly damaged.

V. Conclusion

A multi-physics simulation tool has been developed by coupling 2-D FEM for stress/strain analysis to the previously proposed simulation method of NI REBCO pancake coils based on the PEEC method and 2-D thermal FEA. Multi-physics quench simulations of a 12-stacked NI REBCO single pancake coils were done, and two characteristic phenomena were clarified.

One is that, immediately after the initiate of quench, a small current is induced in the first quenched and the adjacent SP coils due to the simultaneous normal-state propagation in these two SP coils. Another is that, in the bottom SP coil (#12), the increase in the experienced magnetic field induces a current. The increases of current and magnetic field cause the local normal-state transition of SP #12.

Due to these two phenomena, the maximum strains in SPs #2 and #11 are small, and these two SPs are undamaged. No mechanical damage in the second SPs from top and bottom was observed in the experiment of [12]; consequently, the simulation result is in consistency with the experiment. Although we have not yet considered a screening current in this simulation, there is a high possibility that the top and bottom SPs are damaged by high stress due to a screening current.

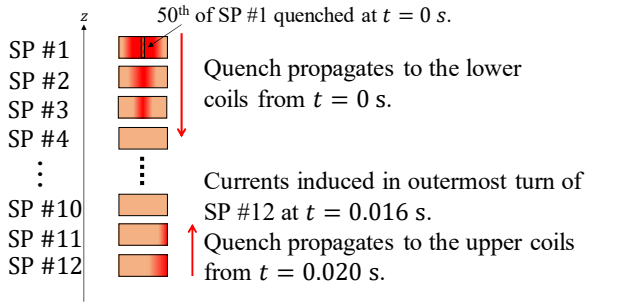

Fig. 8. Mechanism of normal-state propagation from both top and bottom of magnet

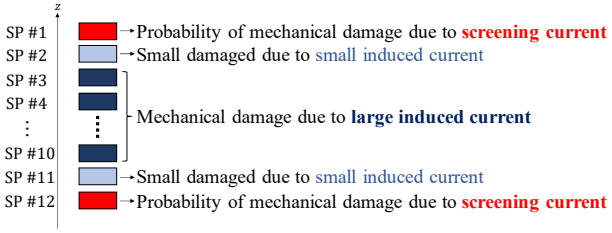

Fig. 9. Mechanical damage factors for each SP in case A.

REFERENCES

[1] S. Hahn, D. K. Park, J. Bascuñán, and Y. Iwasa, "HTS pancake coils without turn-to-turn insulation," *IEEE Trans. Appl. Supercond.*, vol. 21, no. 3, pp. 1592–1595, Jun. 2011.

[2] T. Wang, S. Noguchi, X. Wang, I. Arakawa, K. Minami, K. Monma, A. Ishiyama, S. Hahn, and Y. Iwasa, "Analyses of Transient Behaviors of No-Insulation REBCO Pancake Coils During Sudden Discharging and Overcurrent," *IEEE Trans. Appl. Supercond.*, vol. 25, no. 3, Jun. 2015, Art. no. 4603409.

[3] S. Choi, H. C. Jo, Y. J. Hwang, S. Hahn, and T. K. Ko, "A study on the no insulation winding method of the HTS coil," *IEEE Trans. Appl. Supercond.,* vol. 22, no. 3, Jun. 2012, Art. no. 4904004.

[4] T. Oki, A. Ikeda, T. Wang, A. Ishiyama, S. Noguchi, K. Monma, T. Watanabe, and S. Nagaya, "Evaluation on quench protection for no-insulation REBCO pancake coil," *IEEE Trans. Appl. Supercond.*, vol. 26, no. 4, Jun. 2016, Art. no. 4702905.

[5] Y. Wang, W. K. Chan, and J. Schwartz, "Self-protection mechanisms in no-insulation (RE)$Ba_2Cu_3O_x$ high temperature superconductor pancake coils," *Supercond. Sci. Technol.*, vol. 29, no. 4, Apr. 2016, Art. no. 045007.

[6] J. Xia, H. Bai, H. Yong, H. W. Weijers, T. A. Painter, and M. D. Bird, "Stress and strain analysis of a REBCO high field coil based on the distribution of shielding current," *Supercond. Sci. Technol.*, vol. 32, no. 9, Sep. 2019, Art. no. 095005.

[7] P. Gao, X. B. Wu, C. Xin, T. Liao, W. Wu, and M. Guan, "Numerical investigation on decreasing radial stress in epoxy impregnated REBCO pancake coils by overband," *Cryogenics*, vol. 103, Oct. 2019, Art. no. 102971.

[8] S. Noguchi, "Electromagnetic, thermal, and mechanical quench simulation of NI REBCO pancake coils for high magnetic field generation," *IEEE Trans. Appl. Supercond.*, vol.29, no. 5, Aug. 2019, Art. no. 4602607.

[9] C. Zhou, K. A. Yagotintsev, P. Gao, T. J. Haugan, D. C. van der Laan, and A. Nijhuis, "Critical current of various REBCO tapes under uniaxial strain," *IEEE Trans. Appl. Supercond.*, vol. 26, no. 4, Jun. 2016, Art. no. 8401304.

[10] K. Osamura, S. Machiya, H. Suzuki, S. Ochiai, H. Adachi, N. Ayai, K. Hayashi, and K. Sato, "Reversible strain limit of critical currents and universality of intrinsic strain effect for REBCO-coated conductors," *Supercond. Sci. Technol.*, vol. 22, no. 2, Feb. 2009, Art. no. 025015.

[11] C. Barth, G. Mondonico, and C. Senatore, "Electro-mechanical properties of REBCO coated conductors from various industrial manufacturers at 77 K, self-field and 4.2 K, 19 T," *Supercond. Sci. Technol.*, vol. 28, no. 4, Apr. 2015, Art. no. 045011.

[12] S. Hahn *et al*., "45.5-tesla direct-current magnetic field generated with a high-temperature superconducting magnet," *Nature*, vol. 570, no. 7762, pp. 496–499, Jun. 2019.

[13] P. C. Michael, D. Park, Y. H. Choi, J. Lee, Y. Li, J. Bascuñán, S. Noguchi, S. Hahn, and Y. Iwasa, "Assembly and test of a 3-nested-coil 800-MHz REBCO insert (H800) for the MIT 1.3 GHz LTS/HTS NMR magnet," *IEEE Trans. Appl. Supercond.*, vol. 29, no. 5, Aug. 2019, Art. no. 4300706.

[14] D.Park, J. Bascuñán, P. C. Michael, J. Lee, Y. H. Choi, Y. Li, S. Hahn, and Y. Iwasa, "MIT 1.3-GHz LTS/HTS NMR magnet: post quench analysis and new 800-MHz insert design," *IEEE Trans. Appl. Supercond.*, vol. 29, no. 5, Aug. 2019, Art. no. 4300804.

[15] R. Miyao, H. Igarashi, A. Ishiyama, and S. Noguchi, "Thermal and electromagnetic simulation of multistacked no-insulation REBCO pancake coils on normal-state transition by PEEC method," *IEEE Trans. Appl. Supercond*., vol. 28, no. 3, Apr. 2018, Art. no. 4601405.

[16] S. Noguchi, R. Miyao, K. Monma, H. Igarashi, H. Ueda, and A. Ishiyama, "Current behavior simulation in stacked NI REBCO pancake coils during local normal-state transition," *IEEE Trans. Appl. Supercond*., vol. 27, no. 4, Jun. 2017, Art. no. 4603205.

[17] H. Ueda, Y. Imaichi, T. Wang, A. Ishiyama, S. Noguchi, S. Iwai, H. Miyazaki, T. Tosaka, S. Nomura, T. Kurusu, S. Urayama, and H. Fukuyama, "Numerical Simulation on Magnetic Field Generated by Screening Current in 10-T-Class REBCO Coil," *IEEE Trans. Appl. Supercond*., vol. 26, no. 4, Jun. 2016, Art. no. 4701205.

[18] W. S. Slaughter, *The Linearized Theory of Elasticity*, Basel, Switzerland: Birkhäuser, 2002.

[19] Y. Iwasa, *Case Studies in Superconducting Magnets, Design and Operational Issues*, New York, NY, USA: Springer, 1994.

[20] X. Wang, S. Hahn, Y. Kim, J. Bascuñán, J. Voccio, H. Lee, and Y. Iwasa, "Turn-to-turn contact characteristics for an equivalent circuit model of no-insulation ReBCO pancake coil," *Supercond. Sci. Technol*., vol. 26, no. 3, Mar. 2013, Art. no. 035012.

[21] 2020.[Online]. Available:http://www.superpower-inc.com/content/2g-hts-wire

[22] X. Hu, M. Small, K. Kim, K. Kim, K. Bhattarai, A. Polyanskii, K. Radcliff, J. Jaroszynski, U. Bong, J. H. Park, S. Hahn, and D. Larbalestier, "Analyses of the plastic deformation of coated conductors deconstructed from ultra-high field test coils," *Supercond. Sci. Technol*., vol. 33, no. 9, Sep. 2020, Art. no. 095012.